Published in final edited form as:
*Chem Res Toxicol*. 2010 November 15; 23(11): 1824–1832. doi:10.1021/tx100268g.

# The Metabolism and Toxicity of Menthofuran in Rat Liver Slices and in Rats

**S. Cyrus Khojasteh**[†], **Shimako Oishi**[‡], and **Sidney D. Nelson**[§,*]

[†]Drug Metabolism and Pharmacokinetics, Genentech, Inc., 1 DNA Way MS 412a, South San Francisco, CA 94080 [‡]General Medicine Specialty & Mature Products, Novartis Pharma A.G., Basel, Switzerland [§]Department of Medicinal Chemistry, School of Pharmacy, University of Washington, Box 357610, Seattle, WA 98195

## Abstract

Menthofuran is a monoterpene present in mint plants that is oxidized by mammalian cytochrome P450 (CYP)1 to hepatotoxic metabolites. Evidence has been presented that *p*-cresol and other unusual oxidative products are metabolites of menthofuran in rats, and that *p*-cresol may be responsible in part for the hepatotoxicity caused by menthofuran (Madyastha and Raj, Drug Metabolism and Disposition 20, 295–301, 1992). In the present study, several oxidative metabolites of menthofuran were characterized in rat and human liver microsomes, and in rat liver slices exposed to cytotoxic concentrations of menthofuran. Metabolites that were identified were monohydroxylation products of the furanyl and cyclohexyl groups, mintlactones and hydroxymintlactones, a reactive γ-ketoenal, and a glutathione conjugate. A similar spectrum of metabolites was found in urine 24 hr after the administration of hepatotoxic doses of menthofuran to rats. In no case was *p*-cresol (or any of the other reported unusual oxidative metabolites of menthofuran) detected above background concentrations that were well below concentrations of *p*-cresol that cause cytotoxicity in rat liver slices. Thus, the major metabolites responsible for the hepatotoxic effects of menthofuran appear to be a γ-ketoenal and/or epoxides formed by oxidation of the furan ring.

### Keywords

Menthofuran; toxicity; P450; rat; liver; *p*-cresol

[1]**Abbreviations:** menthofuran, *(R)*-(+)-menthofuran; pulegone, *(R)*-(+)-pulegone; BCA, bicinchoninic acid; BSTFA, *N,O*-bis-(trimethylsilyl)trifluoroacetamide; CI, chemical ionization; CID, collision-induced dissociation; CYP, cytochrome P450; 2D-COSY, 2 dimensional correlation spectroscopy; DLPC, dilauryl-DL-α-phosphatidylcholine; DMSO, dimethylsulfoxide; EI, electron impact; FAB, fast atom bombardment; GC-MS, gas chromatography-mass spectrometry; HEPES, 4-(2-hydroxyethyl)piperazine-1-ethanesulfonic acid; HPLC, high performance liquid chromatography; ISPMS, ionspray mass spectrometry; LDH, lactate dehydrogenase; MFGSH, glutathione conjugate of menthofuran; MFNAC, mercapturic acid conjugate of menthofuran; MLNAC, mercapturic acid conjugate of mintlactone; NMR, nuclear magnetic resonance; rt, retention time; SIM, single ion monitoring; TDC, 5,6,7,8-tetrahydro-4,7-dimethyl-*7H*-cinnoline; TFA, trifluoroacetic acid; TLC, thin layer chromatography; TMCS, trimethychlorosilane; TMS, trimethylsilyl.

CORRESPONDING AUTHOR FOOTNOTE: Tel: 206 543-1419. sidnels@u.washington.edu.

SUPPORTING INFORMATION PARAGRAPH. More information is available on synthesis and characterization of metabolites in the Supportment.

## INTRODUCTION

*(R)*-(+)-Menthofuran (menthofuran) (**1**, Figure 1) is a monoterpene present in mint plants, and it also is formed as a mammalian metabolite of the monoterpene, *(R)*-(+)-pulegone (pulegone) (1–3). Pulegone is abundant in pennyroyal, a mint plant whose products have been associated with toxicity in humans (4,5), and menthofuran has been shown to be the major proximate hepatotoxic metabolite of pulegone in rats (6). Furans, in general, are a class of compounds that are susceptible to oxidative metabolism by cytochrome P450 (CYP) enzymes (7). Oxidative cleavage of the furan ring has been documented (8–18), and γ-ketoenal or enedial metabolites have been identified as reactive intermediates in some cases (10,13–19), including (Z)-(2'-keto-4'-methylcyclohexylidene) propanal, the γ-ketoenal (Figure 1) of menthofuran (13–15). Pulegone and menthofuran also are metabolized to diastereomeric mintlactones (**6, 7**) and hydroxymintlactones (**8, 9**) (15,20–23), a furanyl glutathione conjugate (21,22,24), and a series of cleavage products that ultimately yield *p*-cresol and benzoic acid (25) (refer to Figure 1 for structures).

The major aim of the work presented in this report was to determine which metabolites of menthofuran are most responsible for hepatotoxicity in rats. In particular, we wanted to determine if *p*-cresol was formed from menthofuran in amounts sufficient to cause hepatotoxicity.

Although our previous studies, using semicarbazide to trap the γ-ketoenal as its 5,6,7,8-tetrahydro-4,7-dimethyl-7*H*-cinnoline (TDC) condensation product, showed that the γ-ketoenal was the major reactive metabolite of menthofuran that bound to mouse, rat and human liver microsomes (15), semicarbazide could not be used in studies *in vivo* as an aid in defining the role of the γ-ketoenal in hepatotoxicity caused by menthofuran. Therefore, we investigated the utility of rat liver slices as a model for hepatocellular injury where various treatments and trapping agents could be used to assess their effects on toxicity. In addition, the metabolism of menthofuran was further investigated in rat and human liver microsomes, rat liver slices, and in rats *in vivo*.

Results of the studies indicate that rat liver slices are a useful model to explore mechanisms of hepatocellular injury by menthofuran, and that *p*-cresol was not detected as a metabolite of menthofuran in rat or human liver microsomes, or in rat liver slices or rat urine, consistent with results of similar studies on the metabolism of pulegone (3).

## MATERIALS AND METHODS

### Chemicals

Benzoic acid, *p*-cresol, geraniol, nerol, pyridinium dichromate, sodium chlorite, (*S*)-(−)-perillalcohol, (*S*)-(−)-perillaldehyde and semicarbazide hydrochloride were obtained from Sigma-Aldrich Co. (Milwaukee, WI). [Ring-$d_4$]-*p*-cresol was purchased from Cambridge Isotope Laboratories (Andover, MA). *N*,*O*-Bis-(trimethylsilyl)trifluoroacetamide (BSTFA) containing 1% rimethychlorosilane (TMCS) was purchased from Alltech Associates Inc. (Deerfield, IL). Dimethylsulfoxide (DMSO, HPLC grade), *N*-acetyl-*L*-cysteine, β-glucuronidase/sulfatase type HP-2, D-saccharic acid-1,4-lactone and lactate dehydrogenase (LDH) kit (Lot 22870) were purchased from Sigma Co. (St. Louis, MO). Phenobarbital sodium and British Oxygen Corporation $O_2$/$CO_2$ (95%/5%) were from Shumway Medical Supply (Seattle, WA). All other chemicals were obtained from either Sigma-Aldrich Co. (Milwaukee, WI) or J.T. Baker Chemical Co. (Phillipsburg, NJ) and were of the highest grade available. Liver microsomes were prepared at the University of Washington as previously described (23).

## Instrumentation

$^{1}$H-(300 MHz) and $^{13}$C-(75 MHz) nuclear magnetic resonance (NMR) spectra were recorded in 1,4-dioxane-$d_8$/$D_2O$ or $CDCl_3$ with a Varian VXR-300 spectrometer (Varian Associates Inc., Palo Alto, CA). Standard $^{1}$H-NMR and 2 dimensional correlation spectroscopy (2D-COSY) experiments of a mercapturic acid conjugate of mintlactone (MLNAC) in methanol-$d_4$ were performed with a Bruker (500 MHz) spectrometer. Chemical shifts are reported in ppm (δ) downfield from the internal standard tetramethylsilane.

Thin layer chromatography (TLC) was performed on 2 mm silica gel TLC plates (precoated silica gel 60 $F_{254}$) from Merck (Gibbstown, NJ).

High performance liquid chromatography (HPLC) was performed on a system comprised of two LKB 2150 pumps operated through an LKB 2152 LC controller (LKB, Bromma, Sweden) equipped with a Waters gradient controller. A 5 μm, 10 mm × 250 mm Ultrasphere ODS column was used. Ultraviolet absorbance was monitored online using a Model 450 Waters detector (Millipore, Milford, MA) operating at a wavelength of 254 nm for the glutathione conjugate of menthofuran (MFGSH) and 214 nm for the *N*-acetylcysteine (mercapturic acid) conjugates of menthofuran (MFNAC) and MLNAC. The HPLC mobile phase consisted of 30% methanol in $H_2O$ containing 0.025% trifluoroacetic acid (TFA) (Solvent A) and 95% methanol containing 0.025% TFA (Solvent B). The gradients used for isolation of the *N*-benzyloxycarbonyl derivative of MFGSH and MLNAC were as follows, respectively: (1) a linear increase of 0% Solvent B to 100% Solvent B in 30 min, then for 10 min of Solvent B; (2) 0% Solvent B for 5 min, followed by a linear increase to 100% Solvent B in 45 min. A constant flow rate of 3 mL per min was maintained throughout the analyses. Using gradient (1), MFGSH eluted between 28 and 29 min as detected by its absorption at 254 nm, and was collected in scintillation vials and the frozen sample was lyophilized. The lyophilized sample was analyzed by $^{1}$H-NMR. For mass spectrometric analysis, the lyophilized sample was methylated with methanolic HCl (pH~1), rechromatographed by HPLC, and lyophilized as above. Immediately prior to analysis by ionspray mass spectrometry (ISP-MS) and ionspray tandem mass spectrometry (ISP-MS/MS), the lyophilized sample was reconstituted in methanol/1% aqueous formic acid (1:1, v/v). Using gradient (2), two diastereomeric isomers of MLNAC eluted between 24 and 25 min, and 26 and 27 min, and MFNAC eluted between 28 and 29 min, as detected by absorption at 214 nm. Eluant fractions were collected in scintillation vials and the frozen samples were lyophilized. For mass spectrometric analysis, lyophilized samples were methylated with $CH_2N_2$/diethyl ether.

Fast atom bombardment (FAB) mass spectrometry of MFNAC and MLNAC esters was carried out by adding 1 mL of the methyl esters dissolved in methanol (~10 mM) to a copper stage coated with a liquid matrix of 2-hydroxyethyldisulfide. FAB mass spectra were obtained using a VG70SEQ Tandem Hybrid mass spectrometry equipped with a 1—250 J data system and FAB ion gun. A neutral xenon beam was used at an energy of 8 keV, and the accelerating potential of the ions was 8 kV. Magnetic field scanning from *m/z* 50 to 1200 was repeated at 10 sec intervals. ISP-MS and ISP-MS/MS of the synthetic *N*-benzyloxycarbonyl dimethyl ester of MFGSH, purified by HPLC, was carried out on an Applied Biosystem API III triple quadrupole mass spectrometer (Thornhill, Ontario) equipped with an atmospheric pressure ionization source and an ionspray interface. Full scan mass spectra of the synthetic MFGSH derivative and its corresponding product ion spectra of the $[MH]^+$ ion at *m/z* 618 were generated by direct infusion of the reconstituted HPLC fraction into the mass spectrometer at a flow rate of 5 μL/min. The voltage on the ionspray interface was maintained at 5 kV. High purity air served as the nebulizing gas and was maintained at an operating pressure of 40 p.s.i. High purity nitrogen served as the curtain

gas and was maintained at a constant flow of 1.2 L/min. MS/MS was based on collision-induced dissociation (CID) of the ions entering the rf-only quadrupole region, where argon was used as the target gas at a density of $3.6 \times 10^{14}$ molecules $cm^{-3}$.

Electron impact mass spectrometry (EI-MS) was carried out using a VG-7070H double-focusing instrument (Manchester, UK), equipped with a Hewlett-Packard (Palo Alto, CA) Model 5980 Series II gas chromatograph and online to a Mass Spectrometry Service (Manchester, UK) data system. Injector temperature was 280°C, and splitless injections of 1.0 μL volume were made. Initial column temperature was 60°C, and the temperature was ramped up to 250°C at 10°C/min. The final temperature was held for 10 min. The filament emission current and electron energy were 100 μA and 70 eV, respectively.

Chemical ionization mass spectrometry (CI-MS) was performed in the positive ion mode on a VG Trio-1000 quadrupole instrument (VG Lab-Base software) interfaced to a Hewlett-Packard Model 5980 Series II gas chromatograph with a Hewlett-Packard 7673 autoinjector. Injector temperature was 280°C and splitless injections of 2.0 μL volume were made. The same GC conditions were used as in EI-MS except the final temperature was 280°C. Methane was used as a reagent gas at a pressure of ~1 Torr. Source temperature was 200°C, with a filament emission current of 150 μA and an energy of 70 eV. For quantitative analyses, the mass spectrometer was operated in the selected ion monitoring (SIM) mode with an initial GC temperature of 150°C.

## Synthesis

Syntheses of menthofuran (15), 2-hydroxymenthofuran (23), mintlactone and hydroxymintlactone (15,26), the keto acid (2-[2'-keto-4'-methylcyclohexyl]-propionic acid) (26), TDC (13) and MFGSH (24) have been reported elsewhere. New spectral data for some of these compounds and their trimethylsilyl (TMS) derivatives is reported in the Supporting Information. TMS derivatives were prepared for benzoic acid, 3-methylcyclohexanol, *p*-cresol, hydroxymintlactone, (*S*)-(−)-perill alcohol and (*S*)-(−)-perilla acid. Benzyloxime derivatives of (*R*)-(+)-3-methylcyclohexanone and propionaldehyde were prepared by a previously described method (27). Geranic and neronic acids, and 4- and 5-methyl-2-cyclohexenones, as well as their TMS and oxime derivatives, were synthesized using referenced procedures (28–33) as described in the Supporting Information.

## MFNAC

To 250 mg (1.2 mmol) of α,α'-dimethoxydihydromenthofuran in 14 mL of acetonitrile was added 400 mg (2.5 mmol) of *N*-acetyl-*L*-cysteine and 3 mg (19.4 μmole) of dithiothreitol in 4 mL of distilled water. The reaction mixture was stirred at ambient temperature for overnight under argon gas in a dark room. Acetonitrile was removed under reduced pressure followed by the addition of 10 mL of 1% formic acid. The aqueous solution was subject to solid phase extraction ($C_{18}$), and the desired product was eluted with methanol. After evaporation of methanol at reduced pressure, the sample was frozen in dry ice/acetone and lyophilized. The dried product was purified by preparative TLC using 1-propanol/water/acetic acid (6:3:1 v/v, $R_f$= 0.71) to give 40 mg of MFNAC in 10.7% yield. $^1$H-NMR (methyl ester) (1,4-dioxane-$d_8$/$D_2$0; 4/1) δ 7.15 (d, 1H, *J*= 7.3 Hz, NHCO), 4.55–4.63 (m, 1H Cysα), 3.58 (s, 3H, $COOCH_3$), 3.05 (dd, 1H, *J*= 4.7, 13.8 Hz, Cysβ), 2.96 (dd, IH, *J*= 6.7, 13.7 Hz, Cysβ), 2.64 (dd, 1H, *J*=5.6, 15.9 Hz, H-$7_{eq}$), 2.27–2.32 (m, 2H, H-$4_{ax, eq}$), 2.07–2.18 (m, 1H, H-$7_{ax}$), 1.91 (s, 3H, $CH_3$-3), 1.88 (s, 3H, $NHCOCH_3$), 1.86–1.94 (m, 1H, H-6), 1.76–1.85 (m, 1H, H-$5_{eq}$), 1.25–1.40 (m, 1H, H-$5_{ax}$), 1.05 (d, 3H, *J*=6.5 Hz, $CH_3$-6); $^{13}$C-NMR (methyl ester) (1,4-dioxane-$d_8$/$D_2$0; 4/1) δ 171.3 ($COOCH_3$), 169.2 ($COCH_3$), 153.5 (C-7a), 138.1 (C-2), 127.7 (C-3), 119.3 (C-3a), 52.6 ($COOCH_3$), 52.1 (Cys Cα), 38.2 (Cys Cβ), 31.8 (C-7), 31.6 (C-5), 30.1 (C-6), 22.3 ($COCH_3$), 21.5 (C-9), 20.5 (C-4), 9.3 (C-8); FAB-MS

(methyl ester) *m/z* (% relative intensity) 326 ($[M+H]^+$, 13), 325 ($[M]^+$, 20), 297 ($[M-CO]^+$, 18), 181 ($[M- CH_2CH(NHCOCH_3)CO_2CH_3]^+$, 20), 149 ($[M-SCH_2CH(NHCOCH_3)CO_2CH_3]^+$, 100), 144 ($[CH_2CH(NH_2COCH_3)CO_2CH_3]^+$, 57); GC-CI/MS (methyl ester) *m/z* (% relative intensity) 366 ($[M+C_3H_5]^+$, 6), 354 ($[M+C_2H_5]^+$, 20), 326 ($[M+H]^+$., 40), 183 ($[M+2H-CH_2CH(NHCOCH_3)CO_2CH_3]^+$, 4), 149 ($[M-SCH_2CH(NHCOCH_3)CO_2CH_3]^+$, 100), 144 ($[CH_2CH(NHCOCH_3)CO_2CH_3]^+$, 50), 102 ($[CH_2CH(NH_2)CO_2CH_3]^+$, 6).

## MLNAC

MLNAC was obtained as diastereomeric side products from the synthesis of MFNAC after TLC ($R_f$=0.66). MLNAC was further purified by $C_{18}$-reversed phase HPLC (for conditions, see Instrumentation section). A 2D-COSY NMR of a mixture of the diastereomers of MLNAC showed homonuclear spin coupling between H-6 and H-9, H-5eq and H-5ax, H-7eq and H-7ax, H-4eq and H-4-ax, and H-cysteineα and H-cysteineβ. (Note: Not enough of each individual isomer was available for NMR analysis). For mass spectrometric analysis the compounds were derivatized with $CH_2N_2$. GC-CI-MS (methyl ester) *m/z* (% relative intensities for each of the diastereomers) 382 ($[M+C_3H_5]^+$, 7; 6), 370 ($[M+C_2H_5]^+$, 18; 17), 342 ($[M+H]^+$, 22; 19), 195 ($[M+H-SCH_2CH(NHCOCH_3)CO_2CH_3+C_2H_5]^+$, 5; 7), 178 ($[HSCH_2CH(NHCOCH_3)CO_2CH_3+H]^+$, 100), 167 ([mintlactone+H]$^+$, 31; 44), 165 ($[M-SCH_2CH(NHCOCH_3)CO_2CH_3]^+$, 67; 73), 144 ($[CH_2CH(NHCOCH_3)CO_2CH_3]^+$, 15; 18), 136 ([165 CHO]$^+$, 8; 11), 102 ($[CH_2CH(NH_2)CO_2CH_3]^+$, 17; 25); GC-EI-MS *m/z* (% relative intensity V; VI) 341 ($[M]^{\cdot\bullet+}$, 0; 1), 282 ($[M-CO_2CH_3]^+$, >1; 4), 176 ($[SCH_2CH(NHCOCH_3)CO_2CH_3]^+$, 37; 37), 165 ($[M-SCH_2CH(NHCOCH_3)CO_2CH_3]^+$, 100), 137 ([165 CO]$^+$, 16; 16), 60 ($[HCO_2CH_3]^{\bullet+}$, 15; 30).

## Animals

Rat studies were conducted in accordance with the principles and procedures outlined in the National Institutes of Health National Research Council's Guide for the Care and Use of Laboratory Animals. Male Sprague-Dawley rats (Charles River Inc., Wilmington, MA) weighing from 260 to 280 g were maintained on Wayne Rodent Chow (Animal Specialties, Hubbart, OR) and tap water in a 72 ± 4°F room with 12 hr dark/light cycle. Pretreatment of rats with phenobarbital (80 mg $kg^{-1}$, ip for 4 days) or piperonyl butoxide (1500 mg $kg^{-1}$, ip 30 min prior to killing) were as previously described (13).

Studies with Liver Microsomes from Rats and Humans. Human and rat liver microsomes (0.4 mg protein/incubation) were incubated at 37°C in 250 μL (final volume in 1.5 mL microfuge tubes) of an incubation mixture containing potassium phosphate buffer (100 mM, pH 7.4), $NADP^+$ (0.5 mM), glucose 6-phosphate (10 mM), glucose 6-phosphate dehydrogenase (1 U/mL) and menthofuran (1 mM in 0.01% w/v dilauryl-DL-α-phosphatidylcholine (DLPC) final concentration). Reactions were started by addition of the NADPH-generating system. The reaction mixtures were quenched by placing the tubes in dry ice/acetone. An internal standard of *p*-cresol ring-$d_4$ (10 pmol) was added prior to extraction of each incubation after 5, 15, 30 and 60 min. Samples were extracted with ethyl acetate (100 μL), vortexed for 30 sec, and microfuged for 3 min at 16,000 g. The organic phase was separated and dried over sodium sulfate for analysis. BSTFA (10 μL containing 1% TMCS) was added to 40 μL of extract and incubated for 30 min at 37°C. GC was performed on a Hewlett-Packard 5890 instrument. Chromatography was performed on a 30 mm × 0.32 mm WCOT DB-5 fused silica capillary column (J&W Scientific, Folsom, CA). EI-MS was carried out using a VG Micromass Trio 2000 quadrupole mass spectrometer (Micromass Ltd., Cheshire, UK). The GC temperature program used was as follows. The temperature was kept at 60°C for 3 min and then raised to 120°C final temperature at a constant rate of 10°C/min. The TMS derivative of *p*-cresol eluted at 8.2 min and was

quantified by SIM of the area of the peak at *m/z* 180 divided by the area of peak at *m/z* 184 of its tetra-deuterated standard. The minimum detection limit was 2.5 nM.

Rat Liver Slice Preparation and Incubations. Rats were killed by decapitation after diethyl ether anesthesia and livers were quickly excised. Tissue cores were prepared with a 1 cm outer diameter metal tube and tissue slices (250 ± 25 μm, 30 mg wet weight) were obtained using a mechanical tissue slicer containing ice-cold Krebs-Henseleit buffer (pH 7.4) (34). Slices were incubated in 2.0 mL of Krebs-Henseleit buffer (pH 7.4) supplemented with 25 mM 4-(2-hydroxyethyl)piperazine-1-ethanesulfonic acid (HEPES) at 35°C under a continuous flow of $O_2/CO_2$ (95%/5%) in a shaking water bath. After 45 min preincubation, the tissue slices were transferred into fresh media that contained a final concentration of 0.5 mM menthofuran in DMSO (final media concentration of DMSO was less than 0.5% by volume). Samples were incubated for 6 hr.

Slices for LDH assays were removed at 0, 30, 60, 120 and 360 min after the addition of menthofuran. They were blotted and homogenized in 1 mL of deionized water. After centrifugation of homogenized samples at 10,000 g for 10 min, 100 μL aliquots of the supernatant were diluted with deionized water (1:5), and intracellular LDH activity was determined using Sigma kit 228-10. The activity was expressed as % of control value. LDH activity was normalized to protein content determined using the bicinchoninic acid (BCA) protein assay. Additional 100 μL aliquots of the supernatant were analyzed for *p*-cresol formation as described above for microsomal incubations. After a 30 min incubation with menthofuran, semicarbazide hydrochloride was added to the media of one set of liver slices from untreated rats to obtain final concentrations of 5.0 mM. Control incubations were carried out in the presence of 0.5% DMSO vehicle only.

### Identification of Liver Slice Metabolites

After 6 hr incubation with menthofuran, slices were removed and media from five incubations from each group were pooled. *l*-Menthol (50 nmoles) was added to each 10 mL of incubation medium as an internal standard (I.S.), and metabolites were extracted with an equal volume of ethyl acetate three times. The ethyl acetate layers were dried over anhydrous $Na_2S0_4$, carefully concentrated under a stream of $N_2$ to 40 μL, and derivatized with 10 μL of BSTFA containing 1% TMCS for GC-EI-MS analysis.

### *In Vivo* Urinary Metabolites of Menthofuran

Male Sprague-Dawley rats (260–280 g) received an oral dose of a freshly prepared solution of menthofuran (150 mg $kg^{-1}$) in corn oil. Control rats received vehicle only. Urine was collected into aqueous 1% formic acid solution for 24 hr postdose, and was extracted as described elsewhere (25). Both neutral (pH 7.0) and acidic extracts (pH 1.0) were derivatized as above for GC and GC-EI-MS analysis.

Acid hydrolysis of urine was performed using methods described previously (25). Aliquots (3 mL) of 24 hr urine also were incubated with β-glucuonidase/sulfatase (2800 units of β-glucuronidase and 160 units of sulfatase per mL of urine) in 0.2 M sodium acetate buffer (pH 5.0) for 16 hr at 37°C. For a negative control, β-glucuronidase was preincubated with 2 mM D-saccharic acid-1,4-1actone for 40 min. After hydrolysis, metabolites were extracted with ethyl acetate, dried, derivatized with BSTFA and analyzed by GC-EI-MS.

Mercapturates were isolated by applying aliquots (10 mL) of acidified (pH 1.0) urine, to which was added the trideuterated MFNAC internal standard (100 μM final concentration), to a solid phase extraction cartridge ($C_{18}$). The mercapturates were eluted with methanol, the methanol was removed under reduced pressure, and the sample was lyophilized. To the dried sample, 10 mL of diazomethane/diethylether solution was added and allowed to stand

at ambient temperature for 1 hr. The derivatized samples were taken to dryness and reconstituted in ethyl acetate (200μL) for analysis by GC-CI-MS.

## RESULTS

Lack of Formation of *p*-Cresol in Liver Microsomes. Because *p*-cresol had been reported as a metabolite of menthofuran formed in hepatic microsomes from rats pretreated with phenobarbital (25), and because *p*-cresol is volatile, we developed a GC-EI-MS/SIM stable isotope dilution assay using *p*-cresol-$d_4$ as an internal standard. Although the assay was very sensitive (lowest limit of detection was 2.5 nM), *p*-cresol was not detectable in incubations of menthofuran with liver microsomes at any time point (0, 5, 15, 30 and 60 min) either from untreated or phenobarbital-pretreated rats, or from humans (see Figure S1 in Supporting Information). This translates to no more than 0.00025% conversion of menthofuran to *p*-cresol in any of the microsomal incubations that were carried out under conditions where ~15–30% substrate depletion occurred over the same time period. Other metabolites of menthofuran were formed as previously reported (23).

Toxicity of Menthofuran to Rat Liver Slices. Menthofuran caused a time- and concentration-dependent loss of intracellular LDH when incubated with rat liver slices (Figure 2A). Phenobarbital pretreatment of rats yielded liver slices that showed a significantly increased rate and extent of LDH loss after treatment with menthofuran than liver slices from rats pretreated with the saline vehicle only (Figure 2B). In contrast, piperonyl butoxide, an inhibitor of cytochromes P450, protected liver slices from the toxic effects of menthofuran (Figure 2C). It has been shown previously that semicarbazide condenses with the reactive γ-ketoenal metabolite of menthofuran formed in rat liver microsomes to form TDC (13–15). Here, the addition of semicarbazide to rat liver slices protected cells from the loss of LDH (Figure 2D), with concomitant formation of TDC (Figure 1). This suggests that semicarbazide reacted with the major reactive metabolite(s) and prevented it from eliciting toxicity. The structure of the TDC adduct was confirmed by GC-MS as previously described (13).

Structural Characterization of Metabolites of Menthofuran Formed by Rat Liver Slices. Total ion current chromatograms of TMS derivatized ethyl acetate extracts of the rat liver slice medium, 6 hr after incubation of rat liver slices with menthofuran, revealed the presence of several metabolite peaks (Figure 3A) not found in control incubations (Figure 3B). However, none of the peaks were identified as *p*-cresol, benzoic acid, or any of the other precursors or breakdown products (Figure 1B) reported previously (25). Peaks labeled **1–9** were characterized by analysis of their mass spectra, and in some cases by co-chromatography and mass spectra of synthetic standards. Proposed structures for these metabolites are shown in Figure 1A.

Peak 1 (Figure 3A) was the substrate, menthofuran. Peaks 2–5 all displayed molecular ions at *m/z* 238 and fragment ions at *m/z* 75 and 73 indicating TMS derivatives of monohydroxylated metabolites of menthofuran. Peak 2, a major metabolite formed by incubation of menthofuran with rat liver slices, had a mass spectrum consistent with a furanyl methyl alcohol (see Figure S2 in Supporting Information). This metabolite also was detected as a urinary metabolite of menthofuran, and gave the same mass spectrum.

The mass spectrum of Peak 3 contained fragment ions at *m/z* 196, 181 and 122, the same fragment ions observed in the mass spectrum of the metabolite associated with peak 2 (see Figure S2 in Supporting Information). This indicated hydroxylation at one of the cyclohexyl carbons adjacent to the furan ring that would still allow for retro Diels-Alder elimination of propene from the methylcyclohexyl group. The mass spectrum of Peak 4 showed a base

peak ion at *m/z* 196 with no loss of the trimethylsilyloxy radical (i.e., no fragment ion at m/z 149), suggesting hydroxylation at C-2 of the furan ring. A standard of 2-hydroxymenthofuran has been synthesized (23), and a spectrum of its TMS derivative was found to be identical to that of the TMS-derivatized metabolite in Peak 4. Peak 5 was a metabolite of menthofuran that most likely arose by hydroxylation at C-5, C-6 or C-9 of the cyclohexyl ring inasmuch as the mass spectrum of this metabolite showed no loss of the propene unit. However, the structural assignments are tentative because no standards are available for these latter monohydroxylated products of menthofuran.

Incubation of menthofuran with rat liver slices led to the formation of diastereomeric mintlactones, as well. This was verified by GC-EI-MS analysis of the crude extracts (Peaks 6 and 7 in Figure 3A). Identification of mintlactone and isomintlactone as metabolites was confirmed by comparison of their retention times (13.1 and 13.4 min) and mass spectra with those of synthetic standards, and detailed interpretation of the fragmentation pattern as previously reported (15). Peaks 8 and 9 both had mass spectra identical to the synthetic TMS derivatives of hydroxymintlactone diastereomers (see Supporting Information).

When semicarbazide (5 mM) was added to the incubation medium containing menthofuran (1 mM), and incubated with rat liver slices from untreated rats, cytotoxicity was prevented (Figure 2D) and a compound was formed with a GC retention time and mass spectrum identical to those of synthetic TDC (see Figure 1 for a scheme for TDC formation from menthofuran via its γ-ketoenal reactive metabolite). This is consistent with results using mouse (13), rat 15, 25) and human (15) liver microsomes incubated with menthofuran in the presence of semicarbazide. As another indicator of reactive metabolite formation, a glutathione conjugate of menthofuran was detected as its *N*-benzyloxycarbonyl derivative by ISP-MS/MS (Figure 4) in incubations of menthofuran with rat liver slices without the addition of semicarbazide. The position of glutathione addition was determined by $^{1}$H-NMR (Figure 5) of a standard synthesized as previously described (24). The position was defined by the loss of the signal for the hydrogen at C-2 of the furan ring.

Characterization of Menthofuran Metabolites in Rat Urine. After β-glucuronidase/sulfatase treatment of urine collected for 24 hr after a hepatotoxic dose of menthofuran, several metabolites of menthofuran that had been identified in incubations with rat liver slices were detected as their TMS derivatives by GC-MS analysis of extracts of the treated urine at pH 7.0. All of the monohydroxylated alcohols except 2-hydroxymenthofuran (**4**) were detected, along with the mintlactones (**6 and 7**) and hydroxymintlactones (**8 and 9**) (data not shown). It is not surprising that 2-hydroxymenthofuran was not detected since it tautomerizes to diastereomeric mintlactones, as described previously (23). Diastereomeric keto acids (**10 and 11**) were new metabolites detected as their TMS derivatives in extracts of acidified urine (pH 1.0) after β-glucuronidase/sulfatase treatment (Figure 6). Their structures were confirmed by comparative GC-MS analysis of synthetic standards.

Interestingly, both *p*-cresol and benzoic acid were detected, but they also were found to be present in equivalent amounts in the urine of rats dosed with the corn oil vehicle only (Figure 6). We believe that corn oil is the primary source of *p*-cresol and benzoic acid because naive rats excreted amounts of these substances that were approximately 50-fold less than the amounts found in rats dosed with corn oil (Figure 7).

Since a GSH conjugate of menthofuran was detected in incubations of rat liver slices with menthofuran, and had previously been identified in rat bile after the administration of pulegone (24), scans for daughter ions of methylated mercapturic acids were obtained on urine samples of rats treated with menthofuran. The major mercapturate detected was characterized as MFNAC by comparison of the fragmentation pattern of the methylated

metabolite obtained from rat urine and a deuterated synthetic standard (Figure 8). This deuterated standard was used to quantify the amounts of MFNAC in 24 hr urnie samples of naïve rats treated with a hepatotoxic dose of menthofuran (150 mg/kg), as well as rats pretreated with phenobarbital or piperonyl butoxide prior to treatment with the same hepatotoxic dose of menthofuran. Results showed a significant increase in the excretion of MFNAC in the urine of phenobarbital-treated rats, and a significant decrease in the excretion of MFNAC in rats treated with piperonyl butoxide (Figure 9). These results parallel those of the increases and decreases in hepatotoxicity caused by menthofuran in rat liver slices obtained from rats pretreated with phenobarbital or incubated in the presence of piperonyl butoxide, respectively (Figures 2A–2C).

Two unstable mercapturic acid metabolites also were detected that had a protonated parent ion ($[M+H]^+$ = *m/z* 342) 16 a.m.u, greater than that of MFNAC. They were characterized as disastereomeric mercapturates of mintlactone based on comparisons of their retention times and fragmentation patterns with synthetic standards of MLNAC (Figure 10). These conjugates hydrolyzed in rat urine (pH 7.0) at room temperature to mintlactones, and an NMR spectrum of the synthetic standard showed significant extents of solvolysis (see Figure S3 in Supporting Information for the NMR spectrum).

## DISCUSSION

One of the aims of this investigation was to assess rat liver slices as a model for menthofuran metabolism and toxicity. Menthofuran caused a concentration-dependent increase in LDH leakage from rat liver slices over time that was enhanced by pretreatment of rats with phenobarbital and inhibited by treatment with piperonyl butoxide (Figures 2A–C), treatments previously shown to increase and decrease extents of hepatic necrosis caused by menthofuran *in vivo* (15). In addition, semicarbazide, previously shown to trap a reactive γ-ketoenal metabolite of menthofuran as a TDC derivative (Figure 1) in incubations of menthofuran with liver microsomes from mice, rats and humans (15, 23), trapped the γ-ketoenal metabolite formed from menthofuran in rat liver slices as the same TDC derivative. In parallel, semicarbazide protected the slices from cytotoxicity and LDH release (Figure 2D).

Several other oxidative metabolites of menthofuran were formed in rat liver slices (Figure 3). Most are monohydroxylated products, including 2-hydroxymenthofuran and its tautomeric mintlactones. Hydroxymintlactones also were detected, as well as a glutathione conjugate of menthofuran (Figures 4 and 5). The same metabolites, and/or secondary metabolites derived from them, were found in 24-hr urine samples from rats treated with hepatotoxic doses of menthofuran (Figures 6, and 8–10). These included diastereomeric ketoacids, the 2-mercapturic acid conjugate of menthofuran, MFNAC, and an unstable mercapturic acid, MLNAC, that hydrolyzed to hydroxymintlactones. Some of these compounds have been reported previously as metabolites formed from pulegone and menthofuran *in vitro* and *in vivo* in mice and rats (2,3,21–25). In addition, sulfonic acid and glucuronide conjugates, formed by sequential metabolism of menthofuran, have been identified and quantified in urine of rats treated with non-hepatotoxic doses of radiolabeled menthofuran (35).

In contrast to some reports (36), *p*-cresol was not detected in incubations of menthofuran with rat or human liver microsomes, or with rat liver slices. A GC-EI-MS/SIM stable isotope dilution assay was used that was sensitive to concentrations of *p*-cresol in the low nanomolar range. Since near mM concentrations of *p*-cresol are required for hepatocellular injury in rat liver slices (37), it is unlikely that *p*-cresol is a significant contributor to the hepatotoxicity of menthofuran. Although it is known that *p*-cresol is oxidized to reactive

metabolites by CYP enzymes (38), it is not oxidized rapidly, and it is a major compound detected in serum and urine after the administration of *p*-cresol *in vivo* (39,40). Therefore, we should have been able to detect *p*-cresol itself in our incubations, if it were formed. Furthermore, although *p*-cresol and another proposed oxidation product of menthofuran, benzoic acid (25,36) were detected in naïve rat urine and in ~50x those concentrations after the administration of menthofuran, they also were detected in the urine of rats treated with the corn oil vehicle only, in the same quantities as in the urine of rats treated with menthofuran (Figure 6).

We do not have an explanation for why our results differ from those reported previously (14,25,36). These investigators detected several compounds in incubations of menthofuran with rat liver microsomes and in urine of rats dosed with menthofuran that could arise from an unusual set of furan ring oxidations, fragmentations and rearrangements. In addition to *p*-cresol and benzoic acid, the compounds detected (as shown in Figure 1, Panel B) were perill alcohol and acid, 5-methylcyclohexanone, 5- and 4-methyl-2-cyclohexen-1-ones, 3-methylcyclohexanol, geranic and neronic acids, and propionaldehyde (see Supporting Information for their syntheses and GC-EI-MS characterization as either TMS or benzyloxime derivatives). However, we did not detect above low background levels any of these novel cleavage products. Based on (i) previous characterization of a γ-ketoenal as a reactive metabolite of menthofuran (3,13–15,21,23), (ii) results of studies reported herein that semicarbazide protected rat liver slices from hepatocelluar damage with comcomitant formation of TDC as the semicarbazide-trapped γ-ketoenal, and (iii) detection of GSH-derived products of oxidative metabolites of menthofuran in rat liver slices and rat urine, we conclude that the ultimate hepatotoxic metabolites of menthofuran arise from initial oxidation of the furan ring to a furanyl epoxide and/or a γ-ketoenal, and not from *p*-cresol.

## Supplementary Material

Refer to Web version on PubMed Central for supplementary material.

## Acknowledgments

This work was support by National Institute of Health Grants GM 25418 (to S.D.N.), Program Project Grant GM 32165, and the UW NIEHS sponsored Center for Ecogenetics and Environmental Health Grant P30ES07033.

## REFERENCES

1. Gordon WP, Huitric AC, Seth CL, McClanahan RH, Nelson SD. The metabolism of the abortifacient terpene, (*R*)-(+)-pulegone to a proximate toxin, menthofuran. Drug Metab. Dispos. 1987; 15:589–594. [PubMed: 2891472]
2. Moorthy B, Madyastha P, Madyastha KM. Metabolism of a monoterpene ketone, *(R)*-(+)-pulegone, a hepatotoxin in rat. Xenobiotica. 1989; 19:217–224. [PubMed: 2728495]
3. Chen LJ, Lebetkin EH, Burka LT. Metabolism of *(R)*-(+)-pulegone in F344 rats. Drug Metab. Dispos. 2001; 29:1567–1577. [PubMed: 11717176]
4. Anderson IB, Mullen WH, Meeker JE, Khojasteh-Bakht SC, Oishi S, Nelson SD, Blanc PD. Pennyroyal toxicity: Measurement of toxic metabolite levels in two cases and review of the literature. Ann. Intern. Med. 1996; 124:726–734. [PubMed: 8633832]
5. Bakerink JA, Gospe SM Jr, Dimand RJ, Eldridge MW. Multiple organ failure after ingestion of pennyroyal oil from herbal tea in two infants. Pediatrics. 1996; 98:944–947. [PubMed: 8909490]
6. Thomassen D, Slattery JT, Nelson SD. Contribution of menthofuran to the hepatotoxicity of pulegone: Assessment based on matched area under the curve and on matched time course. J. Pharmacol. Exp. Ther. 1988; 244:825–829. [PubMed: 3252034]
7. Burka, LT.; Boyd, MR. Furans. In: Anders, MW., editor. Bioactivation of Foreign Compounds. Orlando: Academic Press; 1985. p. 243-257.

8. Trudgill PW. The metabolism of 2-furoic acid by Pseudomonas F2. Biochem. J. 1969; 113(4):577–587. [PubMed: 4318274]
9. Frank A. Studies on the metabolism of 2-(2-furyl) benzimidazole in certain mammals. Acta. Pharmacol Toxicol. 1971; 29 Suppl 2:80–124.
10. Ravindranath V, Burka LT, Boyd MR. Reactive metabolites from the bioactivation of toxic methylfurans. Science. 1984; 224(4651):884–886. [PubMed: 6719117]
11. Le Fur JM, Labaune JP. Metabolic pathway by cleavage of a furan ring. Xenobiotica. 1985; 15(7): 567–577. [PubMed: 4049897]
12. Kobayashi T, Sugihara J, Harigaya S. Mechanism of metabolic cleavage of a furan ring. Drug Metab. Dispos. 1987; 15:877–881. [PubMed: 2893716]
13. McClanahan RH, Thomassen D, Slattery JT, Nelson SD. Metabolic activation of *(R)*-(+)-pulegone to a reactive enonal that covalently binds to mouse liver proteins. Chem. Res. Toxicol. 1989; 2:349–355. [PubMed: 2519826]
14. Madyastha KM, Raj CP. Biotransformations of R-(+)-pulegone and menthofuran in vitro: Chemical basis for toxicity. Biochem. Biophys. Res. Commun. 1990; 173:1086–1092. [PubMed: 2268314]
15. Thomassen D, Knebel N, Slattery JT, McClanahan RH, Nelson SD. Reactive intermediates in the oxidation of menthofuran by cytochromes P-450. Chem. Res. Toxicol. 1992; 5:123–130. [PubMed: 1581528]
16. Chen LJ, Hecht SS, Peterson LA. Identification of cis-2-butene-1-4-dial, as a microsomal metabolite of furan. Chem. Res. Toxicol. 1995; 8:903–906. [PubMed: 8555403]
17. Zhang KE, Naue JA, Arison B, Vyas KP. Microsomal metabolism of the 5-lipoxygenase inhibitor L-739,010: Evidence for furan bioactivation. Chem. Res. Toxicol. 1996; 9:547–554. [PubMed: 8839061]
18. Sahali-Sahly Y, Balani SK, Lin JH, Baillie TA. In vitro studies on the metabolic activation of the furanopyrimidine L-754,394, a highly potent and selective mechanism-based inhibitor of cytochrome P450 3A4. Chem. Res. Toxicol. 1996; 9:1007–1012. [PubMed: 8870989]
19. Peterson LA, Cummings ME, Chan JY, Vu CC, Matter BA. Identification of a cis-2-butene-1,4-dial-derived glutathione conjugate in the urine of furan-treated rats. Chem. Res. Toxicol. 2006; 19:1138–1141. [PubMed: 16978017]
20. Madyastha KM, Raj CP. Studies on the metabolism of a monoterpene ketone, R-(+)-pulegone -- a hepatotoxin in rat: Isolation and characterization of new metabolites. Xenobiotica. 1993; 23:509–518. [PubMed: 8342298]
21. Chen LJ, Lebetkin EH, Burka LT. Comparative disposition of *(R)*-(+)-pulegone in B6C3F1 mice and F344 rats. Drug Metab. Dispos. 2003; 31:1–8. [PubMed: 12485945]
22. Ferguson LJ, Lebetkin EH, Lih FB, Tomer KB, Parkinson HD, Borghoff SJ, Burka LT. 14C-labeled pulegone and metabolites binding to alpha2u-globulin in kidneys of male F-344 rats. J. Toxicol. Environ. Health A. 2007; 70:1416–1423. [PubMed: 17687727]
23. Khojasteh-Bakht SC, Chen W, Koenigs LL, Peter RM, Nelson SD. Metabolism of *(R)*-(+)-pulegone and *(R)*-(+)-menthofuran by human liver cytochrome P-450s: Evidence for formation of a furan epoxide. Drug. Metab. Dispos. 1999; 27:574–580. [PubMed: 10220485]
24. Thomassen D, Pearson PG, Slattery JT, Nelson SD. Partial characterization of biliary metabolites of pulegone by tandem mass spectrometry: Detection of glucuronide, glutathione, and glutathionyl glucuronide conjugates. Drug Metab. Dispos. 1991; 19:997–1003. [PubMed: 1686249]
25. Madyastha KM, Raj CP. Metabolic fate of menthofuran in rats: Novel oxidative pathways. Drug Metab. Dispos. 1992; 20:295–301. [PubMed: 1352224]
26. Takahashi K, Somcya T, Murald S, Yoshida T. A new ketoalcohol, (−)-mintlactone, (+)-isomintlactone and minor components in peppermint oil. Agric. Biol. Chem. 1980; 44:1535–1543.
27. Devaux PG, Homing MG, Hill RM, Homing EC. O-Benzyloximes: Derivatives for the study of ketosteroids by gas chromatography: Application to urinary steroids of the newborn human. Anal. Chem. 1971; 41:70–80.
28. Corey EJ, Schmidt G. Useful procedures for the oxidation of alcohols involving pyridinium dichromate in aprotic media. Tetrahedron Lett. 1979; 5:399–402.

29. Dalcanale E. Selective oxidation of aldehydes to carboxylic acids with sodium chlorite hydrogen peroxide. J. Org. Chem. 1986; 51:569–571.
30. Frank RL, Hall HK Jr. Monocyclic terpenes from 1,3-diketones. J. Amer. Chem. Soc. 1950; 72:1645–1648.
31. Nystrom RF, Brown WG. Reduction of organic compounds by lithium aluminum hydride. I. Aldehydes, ketones, esters, acid chlorides and acid anhydrides. J. Amer. Chem. Soc. 1947; 69:1197–1199.
32. Birch AJ. Reduction by dissolving metals. Part III. J. Chem. Soc. 1946:593–597.
33. Braude EA, Webb AA, Sultanbawa MUS. Studies in vitamin D field. Part III. Approaches to derivatives of 5-hydroxy-2-methylcyclohexanone. J. Chem. Soc. 1958:3328–3336.
34. Smith PF, Fisher R, Shubat PJ, Gandolfi AJ, Krumdieck CL, Brendel K. In vitro cytotoxicity of allyl alcohol and bromobenzene in a novel organ culture system. Toxicol. Appl. Pharmacol. 1987; 87:509–522. [PubMed: 3564024]
35. Chen LJ, Lebetkin EH, Burka LT. Metabolism of *(R)*-(+)-menthofuran in Fischer-344 rats: Identification of sulfonic acid metabolites. Drug Metab. Dispos. 2003; 31:1208–1213. [PubMed: 12975329]
36. Madyastha KM, Raj CP. Evidence for the formation of a known toxin, p-cresol, from menthofuran. Biochem. Biophys. Res. Commun. 1991; 177:440–446. [PubMed: 2043129]
37. Thompson DC, Pevera K, Fisher R, Brendel K. Cresol isomers: Comparison of toxic potency in rat liver slices. Toxicol. App. Pharmacol. 1994; 125:51–58.
38. Yan Z, Zhong HM, Maher N, Torres R, Leo GC, Caldwell GW, Huebert N. Bioactivation of 4-methylphenol (p-cresol) via cytochrome P450-mediated aromatic oxidation in human liver microsomes. Drug Metab. Dispos. 2005; 33:1867–1876. [PubMed: 16174805]
39. Yashiki M, Kojima T, Miyazaki T, Chiasue F, Ohtani M. Gas chromatographic detection of cresols in the biological fluids of a non-fatal case of cresol intoxication. Forens. Sci. Int. 1990; 47:21–29.
40. Kamijo Y, Soma K, Kokuto M, Ohbu M, Fuke C, Ohwada T. Hepatocellular injury with hyperaminotransferasemia after cresol ingestion. Arch. Pathol. Lab. Med. 2003; 127:364–366. [PubMed: 12653586]

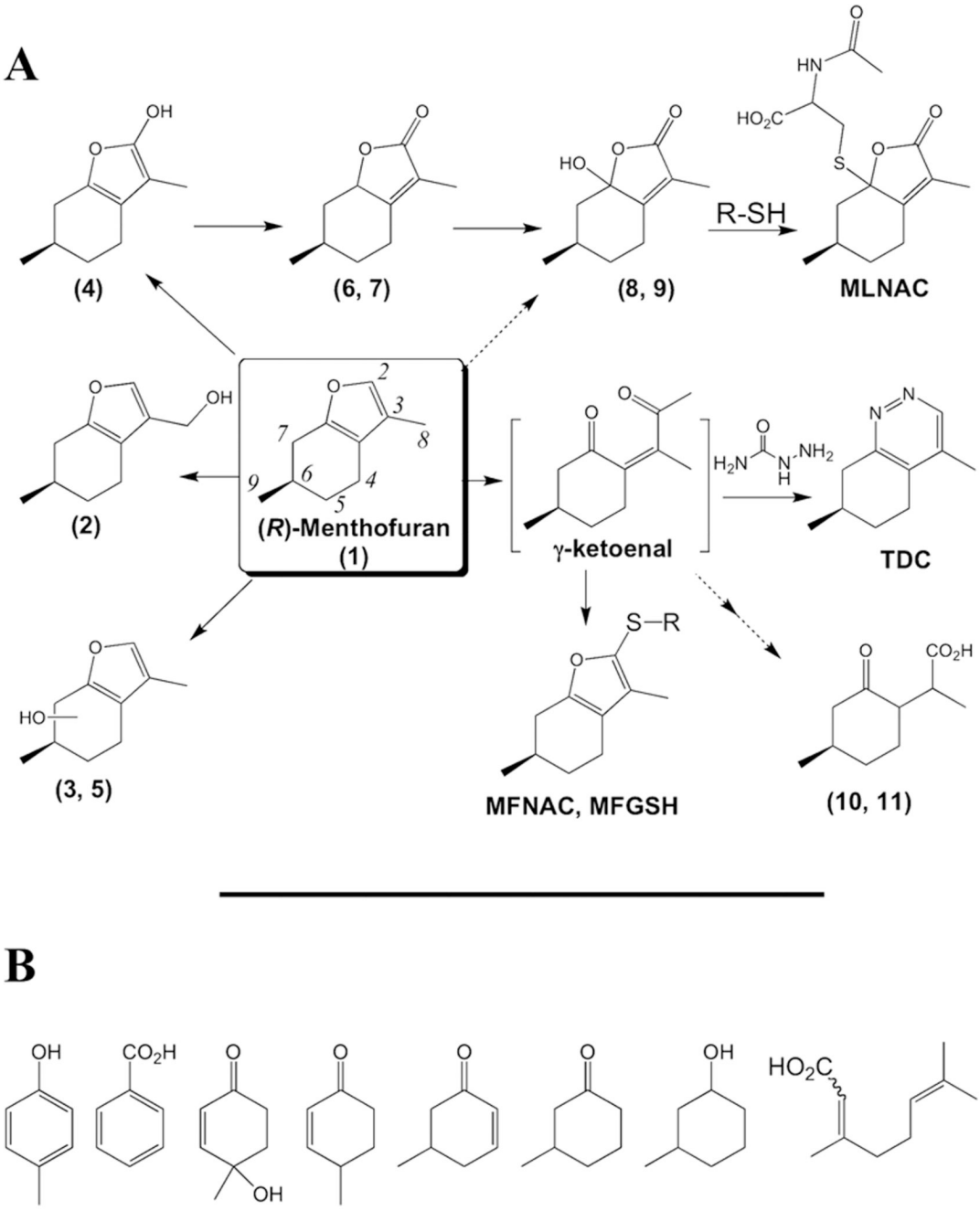


**Figure 1.**

Partial scheme for the metabolism of menthofuran depicting metabolites detected as reported in the present manuscript (Panel A) and some unusual rearrangement products reported elsewhere (Panel B). Note that TDC is formed by condensation of the two hydrazide nitrogens with the enonal carbonyls of the γ-ketoenal intermediate, followed by dehydration and decarbamylation as reported previously (13).

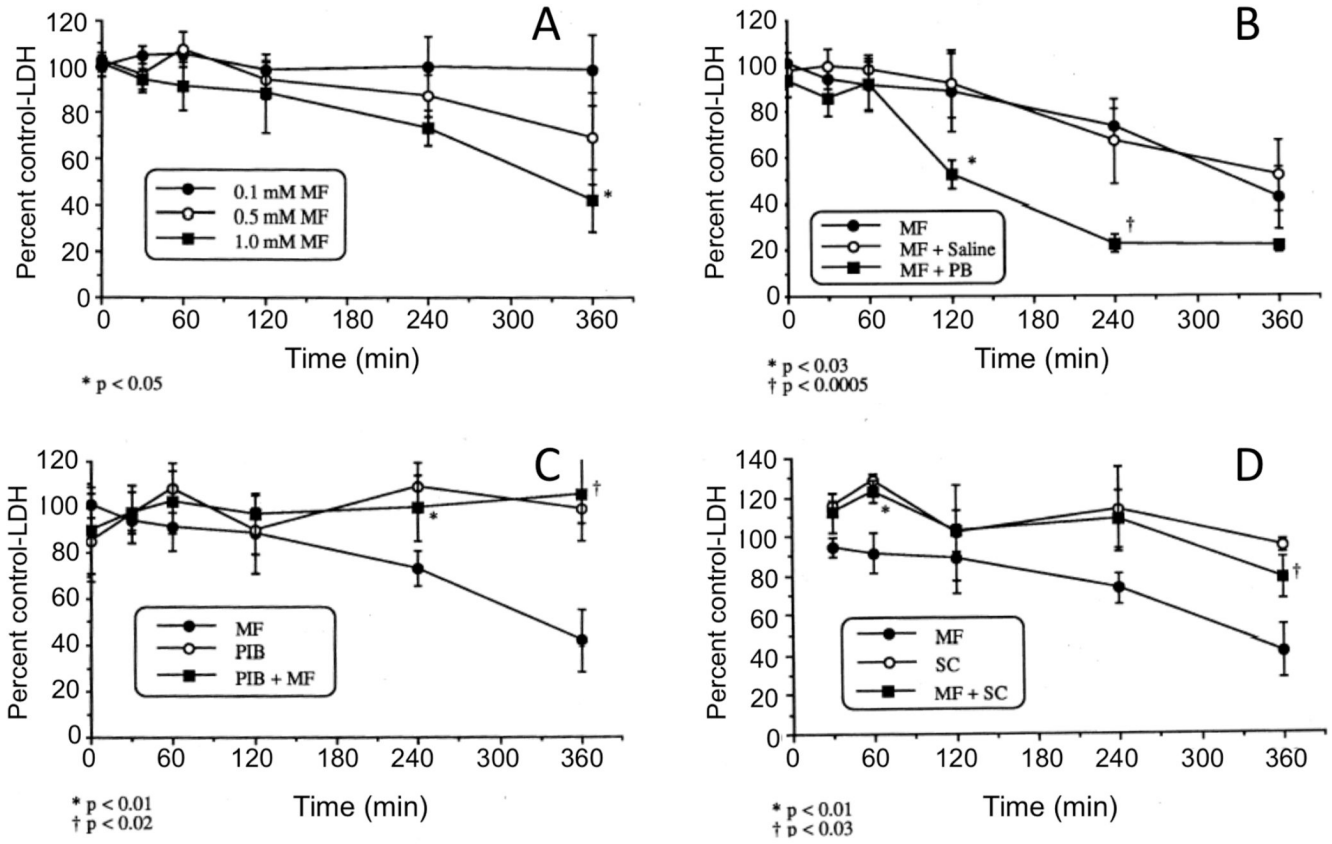


**Figure 2.**

Cytotoxicity in rat liver slices as assessed by monitoring LDH activity in liver slice cells. Panel A: Effect of menthofuran (MF) concentration over time on the loss of LDH activity from liver slices obtained from naïve rats. Panel B: Effect of phenobarbital pretreatment of rats on the loss of LDH activity over time from liver slices treated with menthofuran (1.0 mM). Panel C: Effect of piperonyl butoxide (PIB, 1.0 mM) on the loss of LDH activity over time from rat liver slices treated with menthofuran (1.0 mM). Panel D: Effect of semicarbazide (5.0 mM) on the loss of LDH activity over time from rat liver slices treated with menthofuran (1.0 mM).

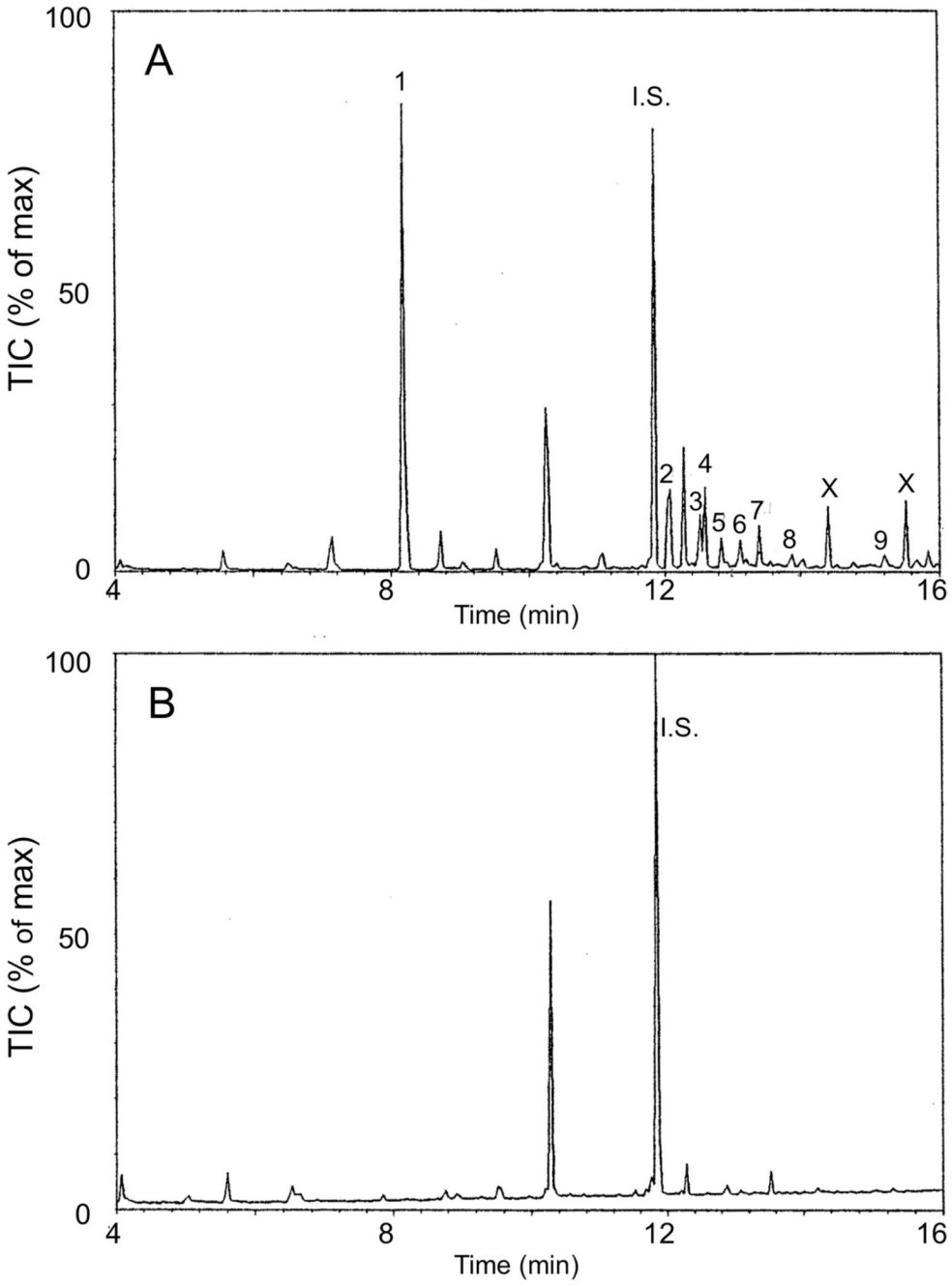


**Figure 3.**

GC-MS profiles of silylated ethyl acetate extracts from rat liver slice incubations with (A) 0.5 mM menthofuran/DMSO and (B) with DMSO only. The final concentration of DMSO was 0.5%. The two peaks marked with an X are of unknown structure, but apparently are the result of multiple oxidations since the major part of their ion current was carried by TMS related peaks. Thus, quantitatively they account for less abundance than they appear in the chromatogram. Refer to Figure 1, Panel A, for structures of the metabolites that correspond to the numbered peaks. Note that neither p-cresol nor benzoic acid were detected in incubations of rat liver slices.

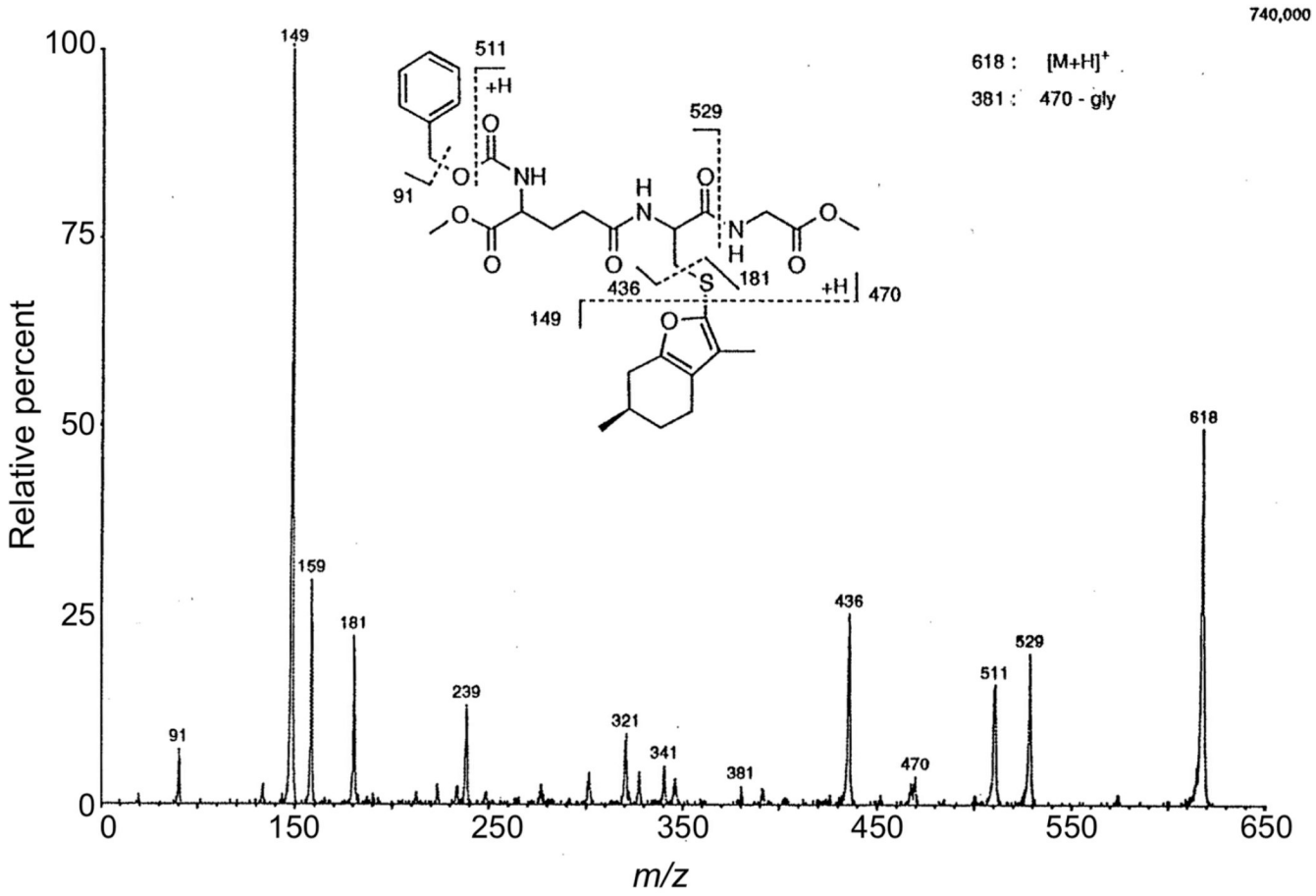


**Figure 4.**
ISP product ion mass spectrum of the $[MH]^+$ ion of the *N*-benzyloxycarbonyl dimethyl ester of MFGSH.

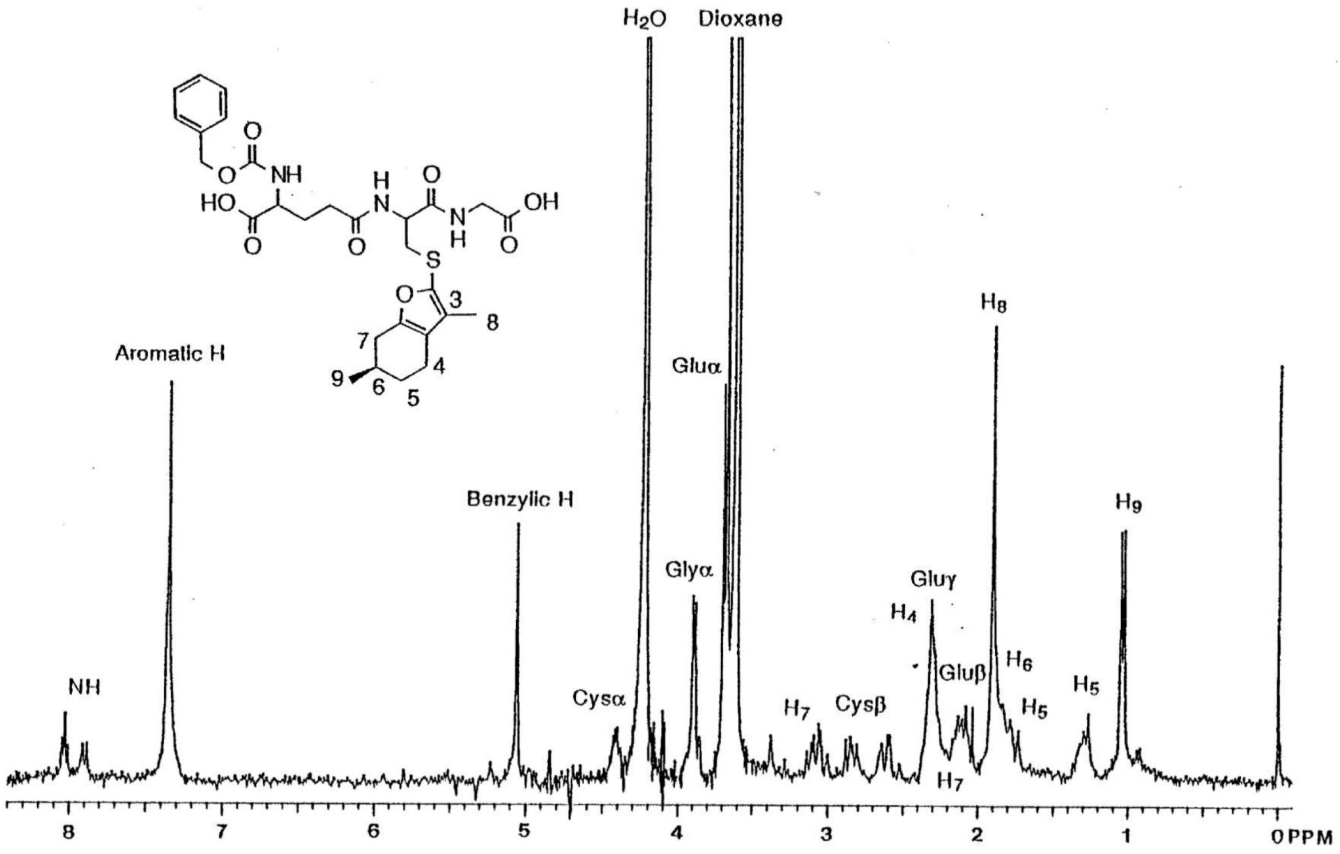


**Figure 5.**
$^{1}$H-NMR spectrum of the *N*-benzyloxycarbonyl derivative of MFGSH in 1,4-dioxane-$d_8$/$D_2O$ (2/1).

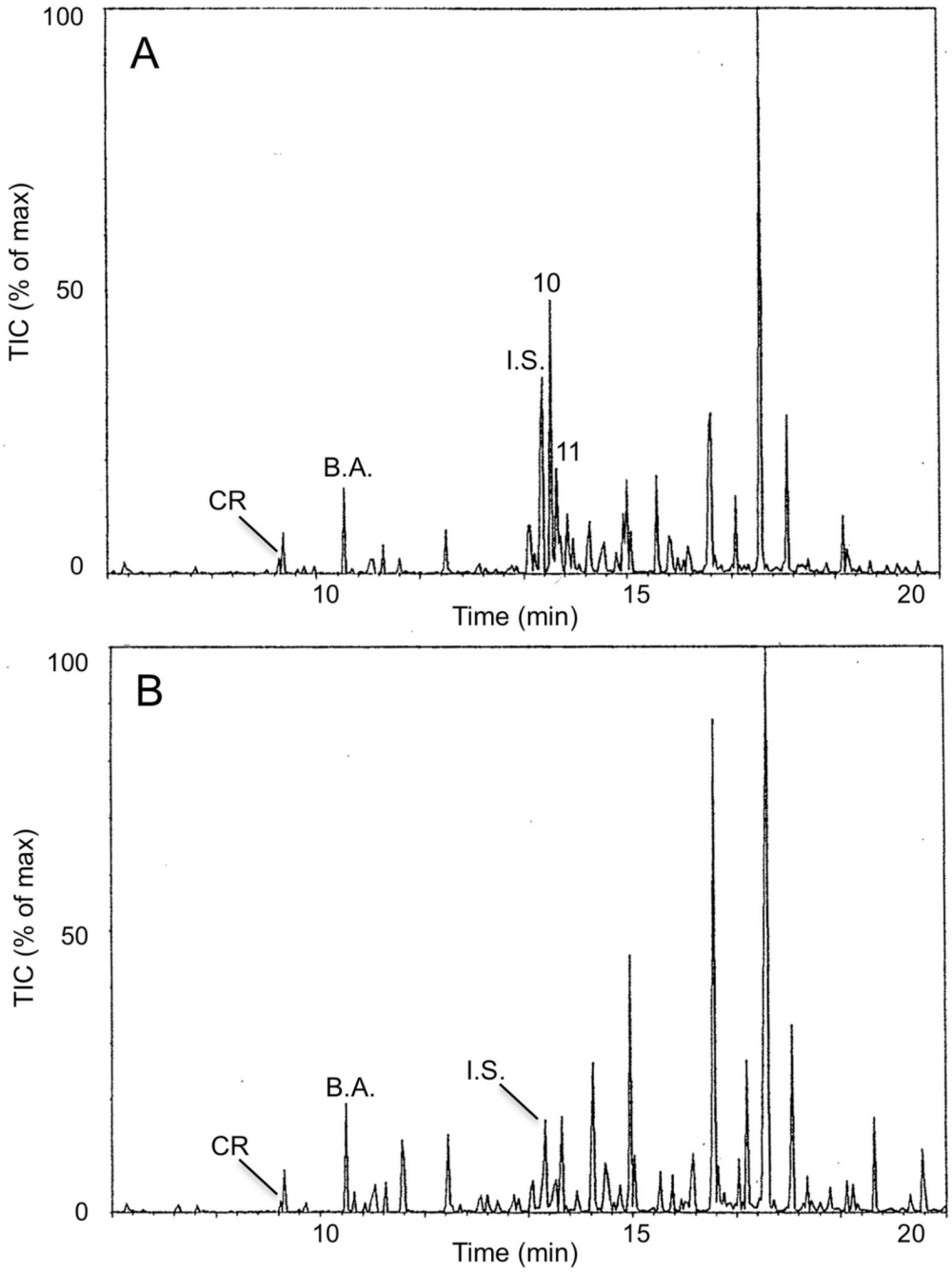


**Figure 6.**

GC-MS analysis of menthofuran and its metabolites as their TMS derivatives in acidified (pH 1.0) urine extracts after β-glucuronidase/sulfatase hydrolysis of urine samples. Total ion current chromatograms from (A) rats dosed with 150 mg/kg menthofuran in 1 mL corn oil and (B) rats dosed with 1 mL corn oil. CR is *p*-cresol, B.A. is benzoic acid, and I.S. is the internal standard, l-menthol, all as their TMS derivatives.

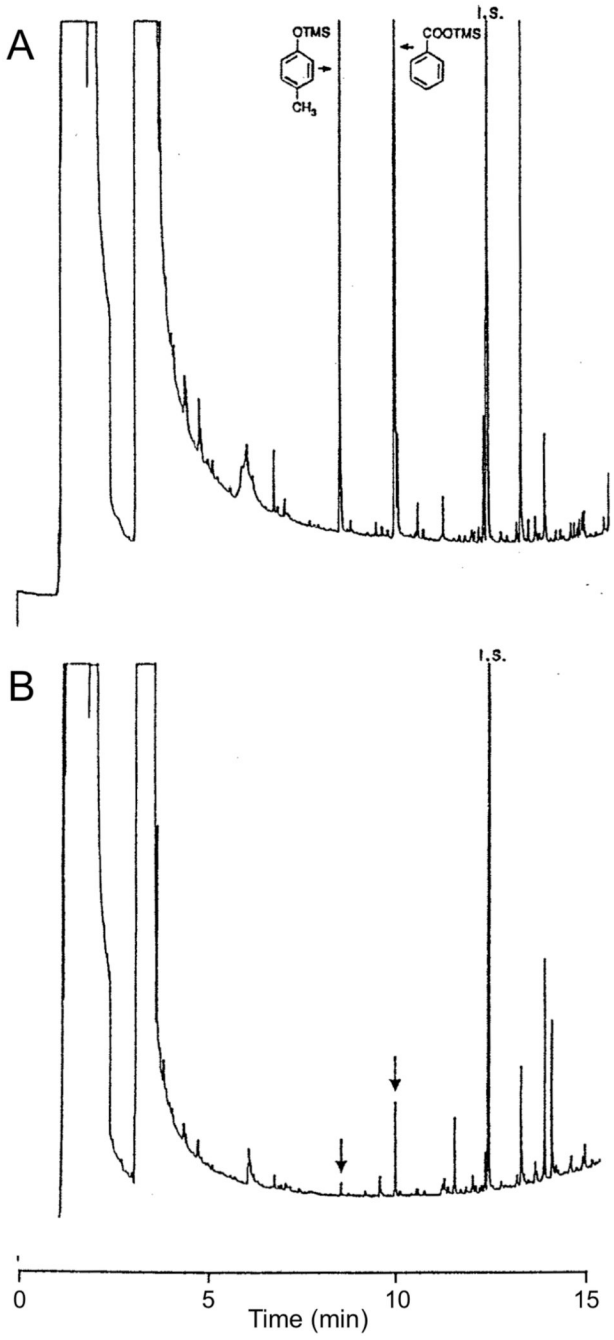


**Figure 7.**
GC analysis of the silylated urine extracts from (A) rats dosed with 1 mL corn oil and (B) naive rats. Urine was treated as described for Figure 6.

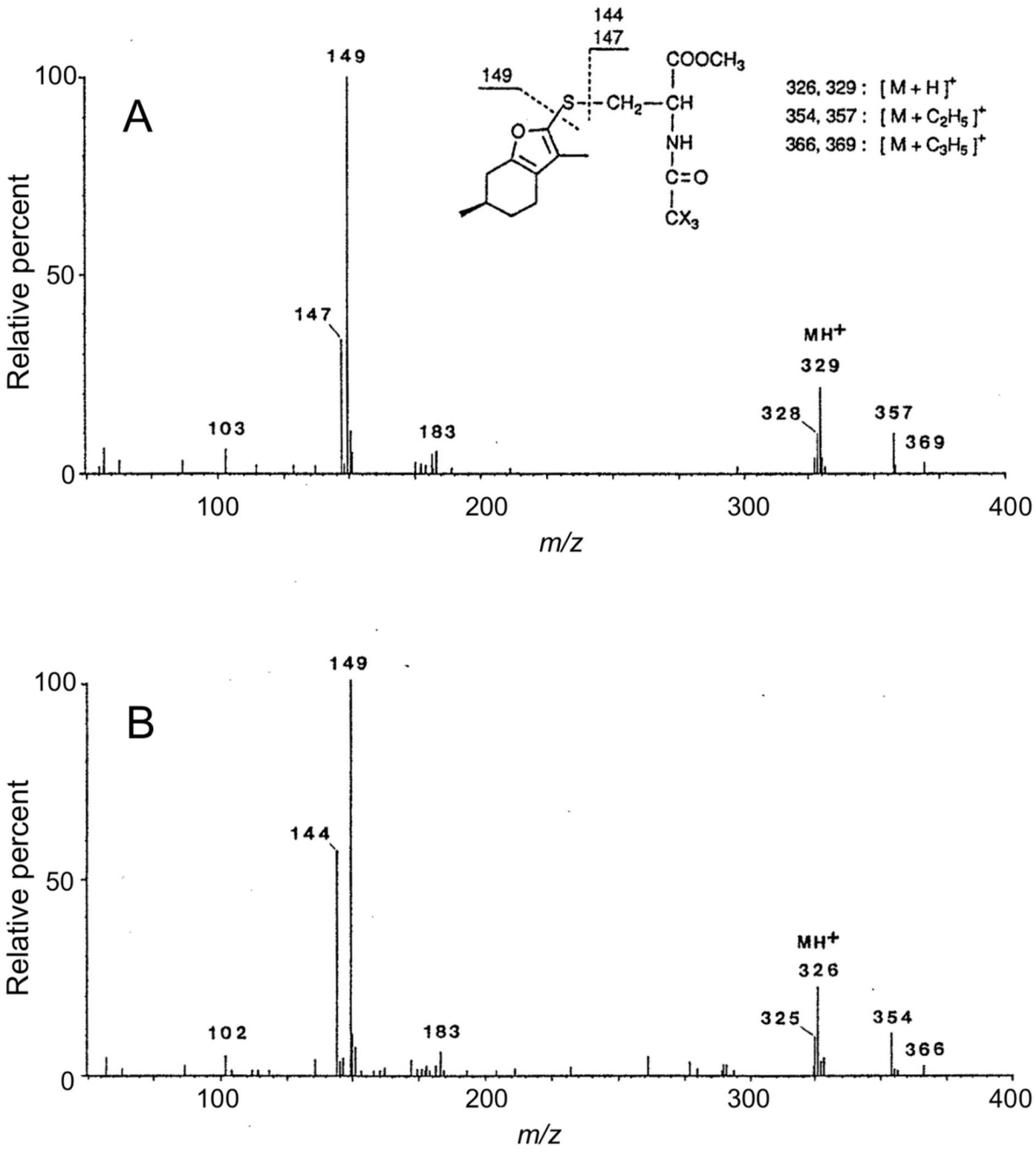


**Figure 8.**
CI-MS of (A) a synthetic deuterated standard of MFNAC methyl ester, and (B) a metabolite from methylated rat urine extracts of rats dosed with menthofuran that had the same GC retention time.

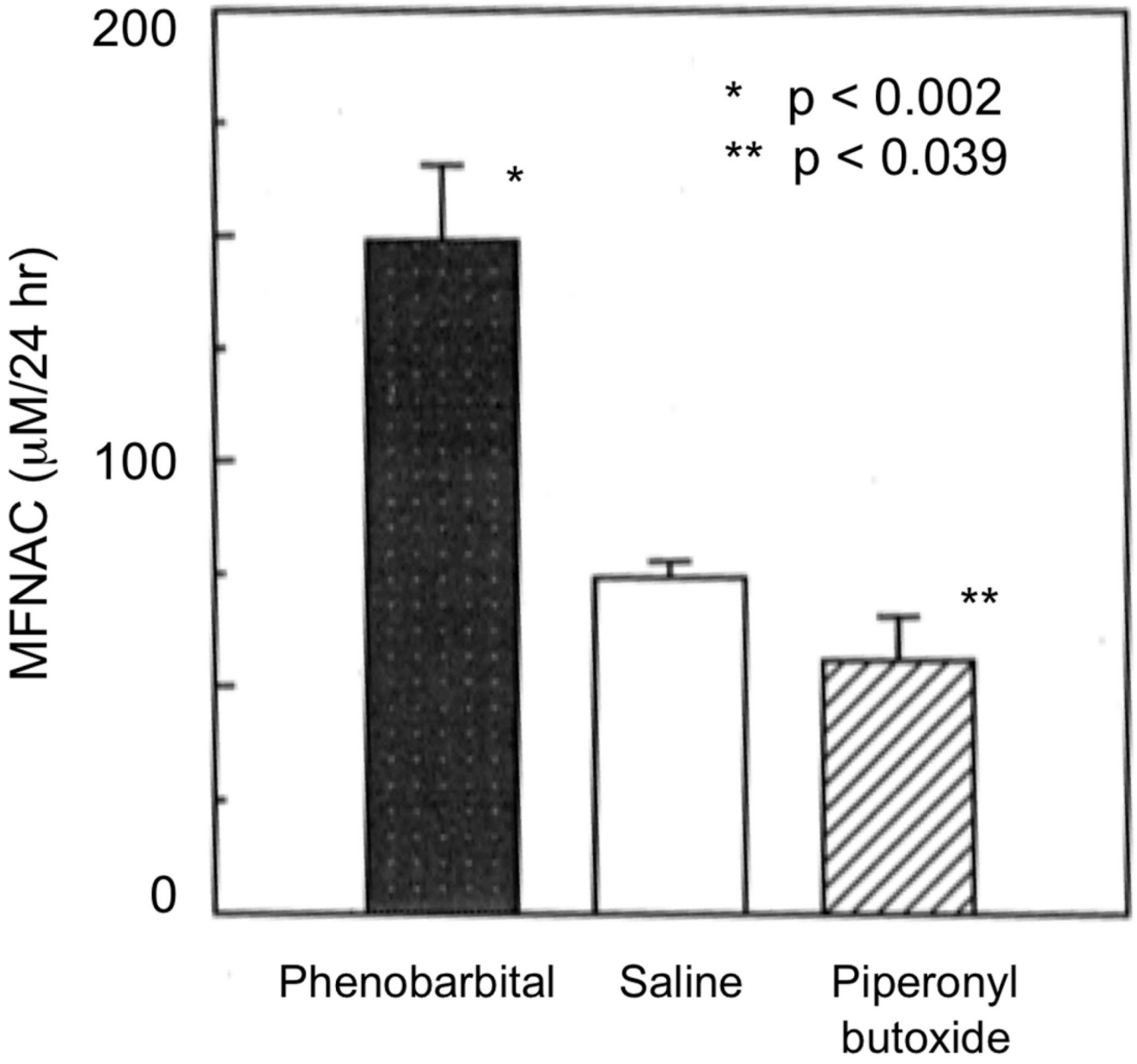


**Figure 9.**

Effects of pretreatment of rats with phenobarbital or the vehicle for injection, saline, and piperonyl butoxide on the amounts of MFNAC appearing in rat urine 24 hr after a dose of 150 mg/kg of menthofuran. Concentrations of MFNAC were determined by GC-CI-MS/SIM of the protonated parent ion of MFNAC methyl ester at m/z 326 compared to the protonated parent ion of its methylated trideuterated internal standard at m/z 329. The trideuterated MFNAC internal standard was added to the urine to give a final concentration of 100 μM prior to isolation and derivatization as described in Materials and Methods. Data are means +/− SD from 4 rats in each treatment group.

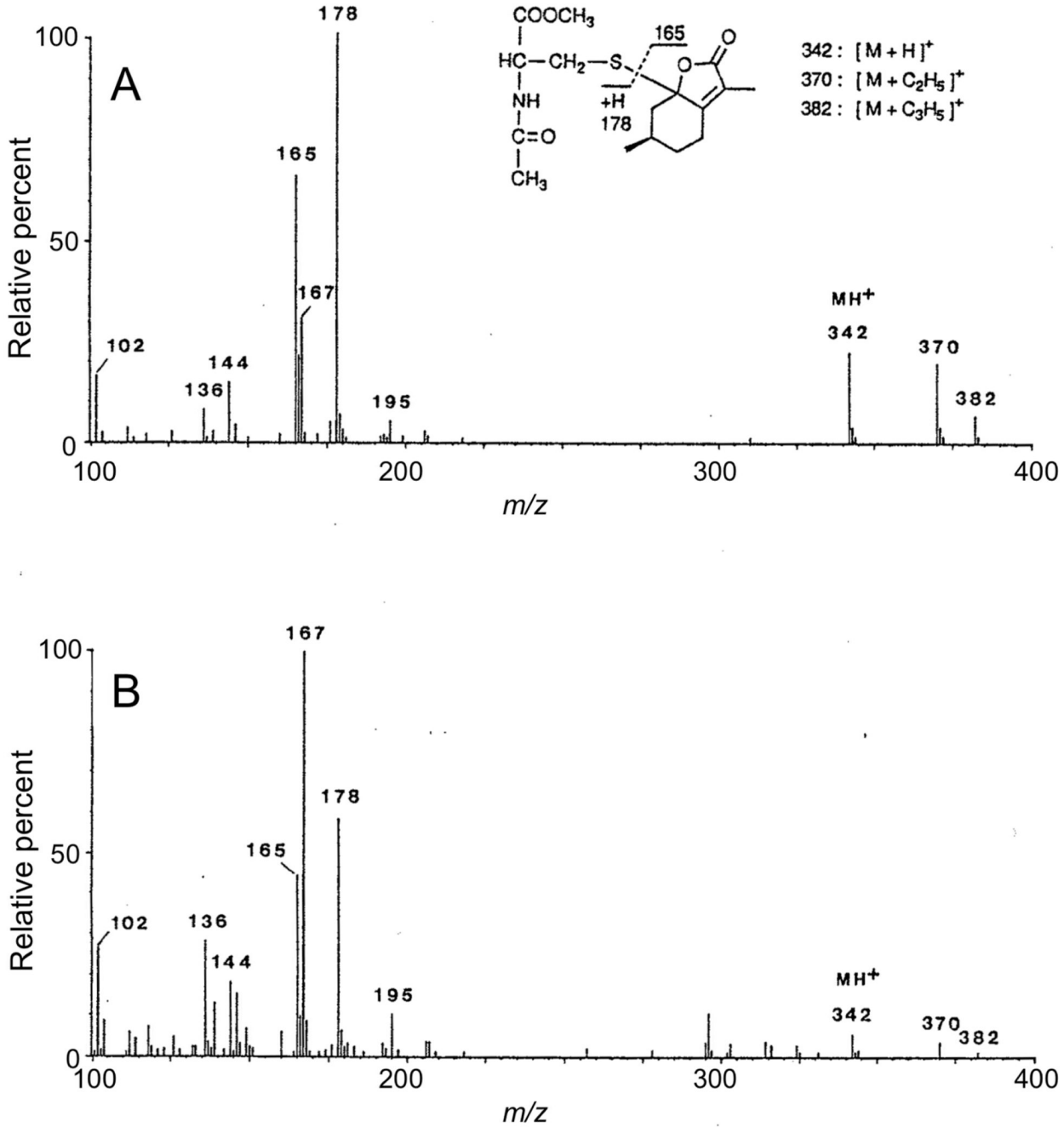


**Figure 10.**

CI-MS of (A) the methylated derivatives of synthetic MLNAC diastereoisomers, and (B) metabolites from methylated rat urine extracts of rats dosed with menthofuran that had the same GC retention times. Isolation and derivatization procedures were the same as described for MFNAC.